

ELECTRON-BEAM TRANSPORT STUDIES FOR RADIOGRAPHIC APPLICATIONS*

D.D. Hinshelwood[‡], D.M. Ponce¹, D. Mosher, D.P. Murphy,
J.W. Schumer, S.D. Strasburg¹, and B.V. Weber

Plasma Physics Division, Code 6773,
Naval Research Laboratory
Washington, DC

Abstract

We have measured electron-beam-produced gas ionization in a paraxial-diode gas cell, using three different interferometric arrangements. We have also measured the beam net current at the channel wall. In the range of tens of kA/cm² and 0.3-5 Torr, the electron density is in the 10¹⁷ cm⁻³ range, scaling strongly with beam current density and sub-linearly with pressure. The fractional net current ranges from 20-40%. We are developing a rate-equation ionization model whose results are consistent with these measurements.

I. INTRODUCTION

The paraxial diode [1] is designed to produce a multi-MV, tens-of-kA electron beam that strikes the anode at near normal incidence. The beam passes into a short cell, rapidly ionizing the neutral gas inside. Because of the finite ionization time, a small self-magnetic field remains in the gas, and this field focuses the electron beam to a small spot. To achieve a small radiographic spot size this field must be tuned, based on the input beam. Because this field is almost impossible to measure inside the beam envelope, a benchmarked modeling capability is crucial. Electron density measurements provide such a benchmark. Electron-density evolution depends on both beam- and plasma-return-current parameters through a number of atomic and molecular processes. Recent measurements of ionization produced by an annular electron beam at current densities in the range of 10 kA/cm² [2] showed discrepancies between measured densities and net currents, with those predicted by the hybrid fluid-PIC code LSP [3]. Such current densities exceed those appropriate to the code's molecular-ionization model. We have begun to develop a rate-equation-based ionization model for LSP appropriate to the higher-current-density regime. The present work provides further data for model benchmarking, and evaluates different interferometric arrangements for paraxial-gas-cell ionization measurements.

II. EXPERIMENTAL ARRANGEMENT

A mock-up of the paraxial diode system was mounted on Gamble II, as shown in Figure 1. Six parallel loads divert most of the 1.4-MV, 700-kA power pulse. About 30-40 kA, are emitted from the 1-cm-diam ball and enter the 3-cm-diam gas cell. The plasma is probed, typically at 3 cm from the anode, by a variety of optical diagnostics. A p-i-n diode array with a rolled edge is also used to diagnose the beam footprint, either at the cell exit (shown), or at the anode plane when the cell is replaced by a solid converter.

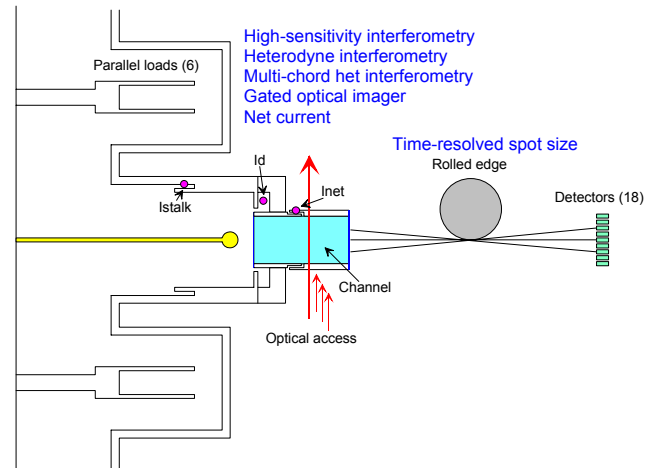


Figure 1. Experimental arrangement on Gamble II.

The rolled-edge data indicate a beam diameter of about 1.2 cm at the anode plane and slightly larger at the channel exit. Beam focusing was not observed and is attributed to a high emittance in the un-optimized incident beam.

As a paraxial-diode mock-up, this work was not intended to address many physics issues. The diode was operated at a similar current, but much lower voltage, than other paraxial diodes. Also, no special care was taken to prevent electron flow upstream of the cathode ball from

* Work supported in part by the US Dept of Energy through Sandia National Laboratories

¹NRC Postdoctoral Research Associate

[‡] email: ddh@suzie.nrl.mil

Report Documentation Page				Form Approved OMB No. 0704-0188	
Public reporting burden for the collection of information is estimated to average 1 hour per response, including the time for reviewing instructions, searching existing data sources, gathering and maintaining the data needed, and completing and reviewing the collection of information. Send comments regarding this burden estimate or any other aspect of this collection of information, including suggestions for reducing this burden, to Washington Headquarters Services, Directorate for Information Operations and Reports, 1215 Jefferson Davis Highway, Suite 1204, Arlington VA 22202-4302. Respondents should be aware that notwithstanding any other provision of law, no person shall be subject to a penalty for failing to comply with a collection of information if it does not display a currently valid OMB control number.					
1. REPORT DATE JUN 2003		2. REPORT TYPE N/A		3. DATES COVERED -	
4. TITLE AND SUBTITLE Electron-Beam Transport Studies For Radiographic Applications				5a. CONTRACT NUMBER	
				5b. GRANT NUMBER	
				5c. PROGRAM ELEMENT NUMBER	
6. AUTHOR(S)				5d. PROJECT NUMBER	
				5e. TASK NUMBER	
				5f. WORK UNIT NUMBER	
7. PERFORMING ORGANIZATION NAME(S) AND ADDRESS(ES) Plasma Physics Division, Code 6773, Naval Research Laboratory Washington, DC				8. PERFORMING ORGANIZATION REPORT NUMBER	
9. SPONSORING/MONITORING AGENCY NAME(S) AND ADDRESS(ES)				10. SPONSOR/MONITOR'S ACRONYM(S)	
				11. SPONSOR/MONITOR'S REPORT NUMBER(S)	
12. DISTRIBUTION/AVAILABILITY STATEMENT Approved for public release, distribution unlimited					
13. SUPPLEMENTARY NOTES See also ADM002371. 2013 IEEE Pulsed Power Conference, Digest of Technical Papers 1976-2013, and Abstracts of the 2013 IEEE International Conference on Plasma Science. IEEE International Pulsed Power Conference (19th). Held in San Francisco, CA on 16-21 June 2013. U.S. Government or Federal Purpose Rights License					
14. ABSTRACT We have measured electron-beam-produced gas ionization in a paraxial-diode gas cell, using three different interferometric arrangements. We have also measured the beam net current at the channel wall. In the range of tens of kA/cm2 and 0.3-5 Torr, the electron density is in the 10¹⁷ cm⁻³ range, scaling strongly with beam current density and sub-linearly with pressure. The fractional net current ranges from 20-40%. We are developing a rate-equation ionization model whose results are consistent with these measurements.					
15. SUBJECT TERMS					
16. SECURITY CLASSIFICATION OF:			17. LIMITATION OF ABSTRACT SAR	18. NUMBER OF PAGES 4	19a. NAME OF RESPONSIBLE PERSON
a. REPORT unclassified	b. ABSTRACT unclassified	c. THIS PAGE unclassified			

entering the diode. LSP simulations indicate that such a non-paraxial flow does occur.

Three different interferometric systems were used to measure the electron density: (1) A Mach-Zehnder setup with active stabilization to increase the sensitivity [4]. The density is given by the arcsine of the detector signal, so that the envelope amplitude is required for calibration. If the plasma density and/or gradients are high enough, a number of effects can reduce or shift this envelope, altering the calibration. (2) A heterodyne interferometer [5], which essentially imposes a series of background fringes on the detector signal. This technique is fairly robust with regard to shifts or reductions in the signal envelope, at the expense of time resolution. (3) A multi-chord heterodyne interferometer, where a ribbon beam traverses the interferometer and is recorded by multiple fiber/detector channels. In this work we used 7 channels spaced over 2 cm across the beam diameter.

III. MEASUREMENTS

The effective time response of the heterodyne system used here is about 20 ns, so this diagnostic is most useful in measuring the peak density at the end of the pulse. Densities are shown in Figure 2 for different pressures of air, along with the beam current. The best radiographic source results [1] were obtained at pressures within this range.

The green curve is a null test with a vacuum ambient. It is a measure of the effect of spurious plasmas from nearby surfaces, and is a worst-case scenario because a gas ambient will tamp emerging plasma.

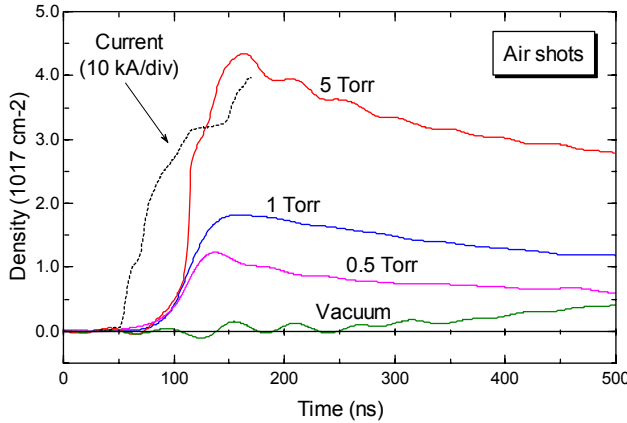


Figure 2. Heterodyne interferometer results.

We see peak line densities in the lower 10^{17} cm^{-2} range. For the path length here, the local density in electrons/ cm^3 is in this range also. The density shows a sub-linear increase with pressure.

We have also looked at helium and argon. Densities with argon are close to those with air. With helium, they are lower: a given density corresponds to a several-fold higher pressure of helium than air, as seen in Figure 3. This is consistent with previous results [1], where

optimum beam transport and focusing with helium occurred at several-fold higher pressures than with air.

A few shots were taken with a reduced Marx charge to change the beam current. Figure 3 shows representative current traces and the resulting densities at the lower current. A slight reduction in current is associated with a steep reduction in density.

The standard and heterodyne systems were fielded together on several shots. Under low-density conditions (low pressure and/or Marx charge) the two agree well at

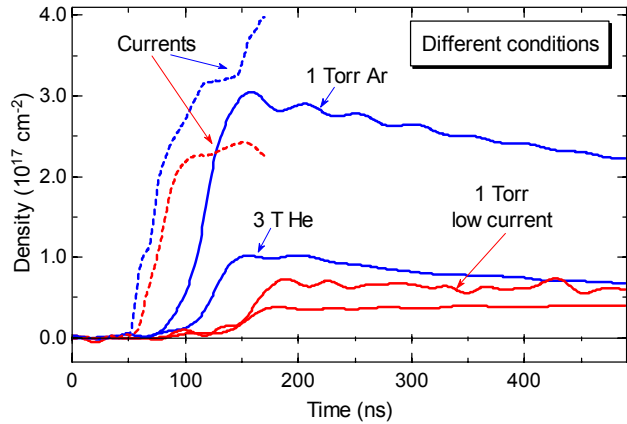


Figure 3. Heterodyne data under different conditions, for comparison with Figure 2.

late times, and at early times the standard signal shows a faster time response. Under high-density conditions, the calculated density values differ greatly. Examination of the heterodyne signal for this case shows that the modulation amplitude decreases sharply during this time. The heterodyne system is relatively unaffected by this but the standard system greatly underestimates the density. For the first part of the pulse, however, the difference is small enough that the standard interferometer data are at least qualitatively valid.

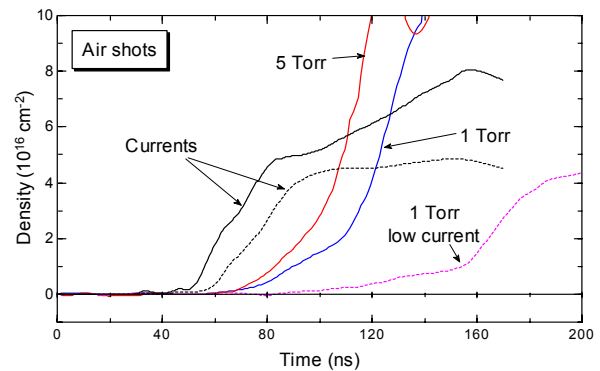


Figure 4. Early-time data obtained by the standard interferometer

These data provide useful information on the electron density evolution. For example, the data in Figure 4 show a transition in the density ramp-up that occurs earlier at

higher pressure. At the lower current, it occurs much later and at a lower current level, suggesting that this transition is related to some integrated quantity, for example the absorbed energy. These data indicate that there are important processes reflected in the density time history. With improved quantitative accuracy and further measurements under different conditions, these physical processes can be better understood. Reproduction of features seen here would be an excellent test of any model.

Figure 5 shows typical data from the multi-chord interferometer. Seven beams traverse the channel in chords spaced over 2 cm. A lineout at the time of peak density is plotted in Figure 6, along with the shape that would be measured for a 1.3-cm diameter uniform channel. The fit is good and allows a straightforward conversion of line density into local, volumetric density.

The indicated channel diameter is consistent with the beam footprints at the anode and channel exit determined from the rolled-edge measurements.

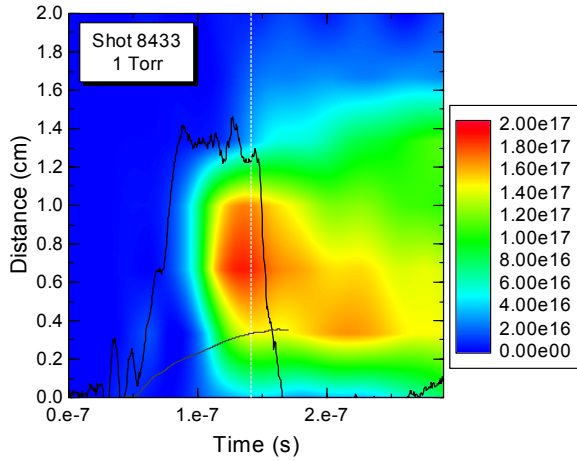


Figure 5. Multichannel heterodyne data. Voltage and current traces are shown superimposed on density data (units of 10^{17} cm^{-2}) as a function of time and distance.

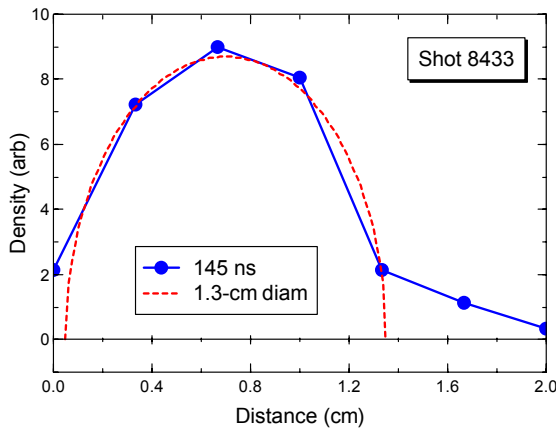


Figure 6. A lineout (solid) of the measured density profile compared with that (dashed) expected from a 1.3-cm-diam uniform channel.

Other measurements show that the channel width at this time is essentially constant over the pressure range from 0.5 to 5 Torr. Later, the width is seen to increase slowly with time. Examination of the 2D data also shows signs of a sideways motion of the density maximum. These effects are important in interpreting the long-timescale density data shown previously: both will lead to an apparent reduction in the calculated local density at the channel center, which could be misinterpreted as recombination.

The net current was measured at the channel wall using a shielded B-dot probe. Figure 7 shows the fractional net current as a function of time for different pressures. The total current and voltage are shown by the dashed curves. As the density drops, the current neutralization improves, reaching a maximum between 1 and .3 Torr. At lower pressures the net current increases abruptly. Even at the minimum, the net current is a finite fraction of the total current.

It is interesting to note that quality of beam focusing obtained in previous experiments [1] follows a very similar pattern: the spot size decreases with pressure to a minimum in the vicinity of 1 Torr, before rapidly increasing as the pressure drops further. This similarity suggests that even better performance may be possible if the net current could be reduced further, for example by replacing the gas ambient with a pre-formed plasma.

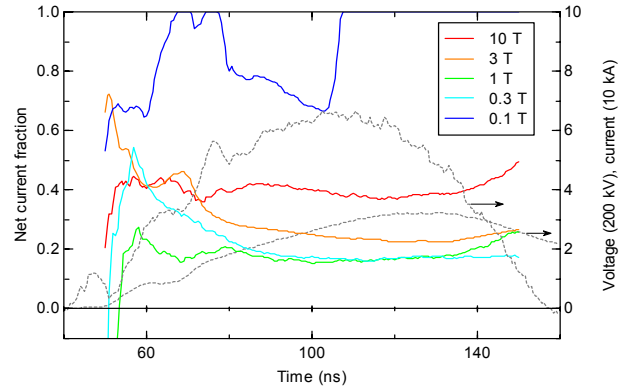


Figure 7. Net current fractions for different pressures, along with the voltage and total current (dashed).

This work has extended the parameter space over which electron density and net current have been measured. Table 1 compares parameters from this work with those from our previous work.

Table 1. Beam parameters

	Paraxial	Annular
Dimensions	1.3-cm diam	1-2cm Δr , 7-cm radius
Current rise	20 kA in 30 ns	800 kA in 60 ns
Current density	15-30 kA/cm ²	7-15 kA/cm ²
Inductive field	1.2 kV/cm	8 kV/cm

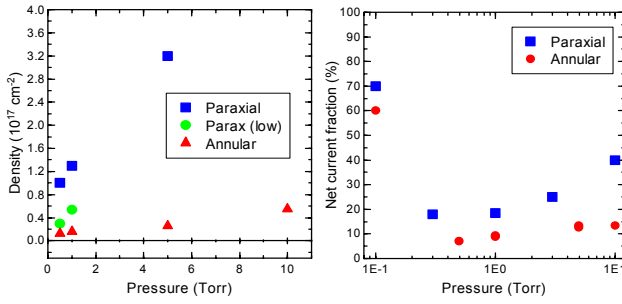


Figure 8. Comparison of electron densities and net currents for the present and previous experiments.

The inductive field refers to the value at the beam edge that would be produced in the absence of current neutralization. Data from the two experiments are compared in Figure 8. The density data are consistent, showing a strong dependence of electron density on beam current density. Both cases show the same functional dependence of net current fraction on pressure. The higher net currents seen in the present work are attributed to the lower inductive field in this case.

IV. RATE EQUATION MODEL

We are developing an ionization model with the goal of producing a module that can be added to LSP. This model combines molecular and atomic rate equations with a coronal ionization model. All processes are included that have significant probability over the relevant timescale. A set of peak-density predictions are shown in Figure 9. These were calculated assuming the current shape from the annular experiments. The current in the present work has a longer effective pulse length.

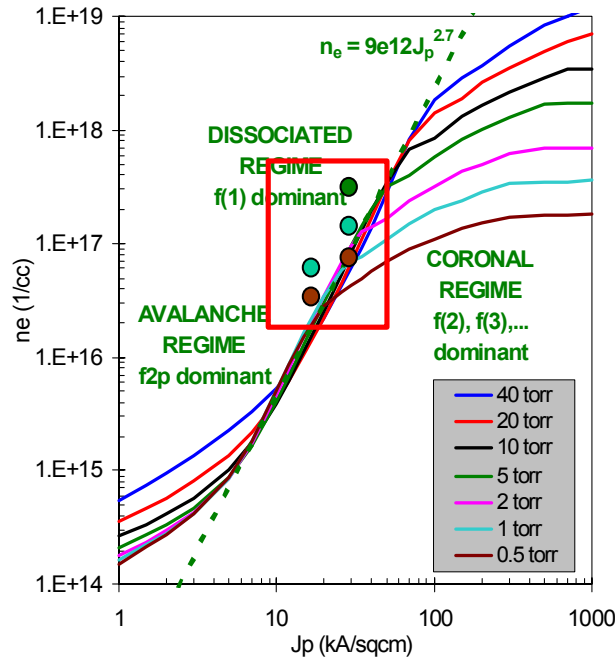


Figure 9. Predictions of the rate-equation model (lines) (for a shorter pulse length than in this work) compared with data from this experiment

This model identifies three regimes: at the lowest current density, the gas is dominated by molecular species, and molecular ionization dominates. At higher current density, the gas is largely dissociated and atomic ionization is more important. Here, recombination can no longer occur by 3-body dissociation, but only by the much slower 2-body radiative process, and the density increases rapidly with current density. At still higher current densities, higher ionization states act as an energy sink and the density increase levels off.

The points inside the box represent the peak densities in this work. They are within a factor of a few of the predicted results. Taking into account the longer effective pulse length will shift these curves to the left, producing even better agreement. Note that in addition to rough quantitative agreement, the model also produces good relative agreement with regard to pressure, and also predicts the sharp fall-off in density with decreasing current observed here. This theory work is ongoing.

V. SUMMARY

We have measured paraxial-gas cell plasma parameters and find peak densities on the order of 10^{17} cm^{-3} . In the range of tens of kA/cm^2 and 0.5-5 Torr, the electron density scales strongly with beam current density and sub-linearly with pressure. We have measured the fractional net current at the channel wall and find minimum values of about 20% at pressures of 0.3-1 Torr. This coincides with the pressure range where optimum focusing was obtained in other experiments. And finally, we have seen good qualitative, and reasonable quantitative agreement with a rate-equation ionization model.

The interferometric diagnostics fielded here provide complimentary information and permit satisfactory measurements of the time- and space-dependent gas ionization. The multi-chord measurement will be particularly useful for experiments where focusing occurs. We are implementing two further improvements: (1) A higher-frequency modulator for the heterodyne system will increase its time response. (2) Converting the standard interferometer to a quadrature system (measuring the sine and cosine simultaneously) will increase its accuracy for large phase shifts.

VI. REFERENCES

- [1] Andrew R. Birrell, et al, IEEE Trans. Plasma Sci., **28**, 1660 (2000).
- [2] S. D. Strasburg, et al, to appear in Physics of Plasmas; also these proceedings.
- [3] D.R. Welch, D.V. Rose, B.V. Oliver, and R.E. Clark, Nucl. Meth. Phys. Res. A **464**, 134(2001).
- [4] B. V. Weber and S. F. Fulghum, Rev. Sci. Instrum., **68**, 1227 (1997).
- [5] B. V. Weber and D. D. Hinshelwood, Rev. Sci. Instrum., **63**, 5199 (1992).